Chapter 6

The Beam Delivery System

6.1 Introduction

At the end of the NLC main linacs, the electron and positron beams have reached their final energy and have typical RMS sizes of 10 μm by 1 μm. The purpose of the beam delivery system (BDS) is to reduce the beams to the sizes required to produce luminosity, remove any particles that are far enough from the beam core to produce unacceptable detector backgrounds, and ensure that the extremely small beams do in fact, collide at the IP. In addition, the BDS must provide protection for the detector and beamline components against missteered beams emerging from the main linacs, and must safely transport the collided beams to water-cooled dumps which can absorb the high beam power density without damage. Finally, the BDS must provide instrumentation that can monitor the parameters of the collided beams, such as the energy spread and polarization after collision, which are required by the particle physics experiments. The four main subsystems of the beam delivery, in order from upstream to downstream, are: the collimation system, which provides protection from errant beams and removes particles which might cause backgrounds; the final focus (FF), which reduces the beam size; the interaction region (IR), which provides detector masking and specialized supports for the final doublet quadrupoles of the final focus; and the extraction line, which transports the spent beams to their respective dumps and provides the post-collision beam measurements.

The beam delivery system is conceptually similar to the low-beta insertion of a colliding-beam storage ring. Because the BDS pushes many of the parameters of a low-beta region to an extreme, its design and implementation are extremely challenging. The horizontal and vertical betatron functions at the IP (β^*_{xy} = 8 x 0.1 mm for 500-GeV cms) are much smaller than those in a storage ring (for example, the PEP-II design betatron functions are 500 x 20 mm). Because the β^* values are so small, the variation of focusing strength with particle momentum, or *chromaticity*, is much larger than in a storage ring and the cancellation of the chromaticity with nonlinear elements must be accomplished with much greater precision. The strong sextupoles which are used to cancel the chromaticity introduce additional high-order aberrations which would enlarge the beam size or reduce the bandwidth of the BDS if not addressed.

Several other issues constrain the design of the BDS. Because the beams at the interaction point (IP) are extremely small, $\sigma^*_{x,y}$ = 245 x 2.7 nm, the beams must collide head-on to within a few nanometers to maintain adequate luminosity. This in turn implies that any source of beam-beam jitter must be strictly limited. The beam-beam focusing at the IP is extremely intense because of the high charge density, which causes the quality of the spent beams to be poor. The energy spread and angular divergence of the outgoing beams at the IP are both large, and a significant fraction of the beam power is converted to photons in the collision. The number of particles in the beam 'halo' which are far from the core and can cause backgrounds can potentially be quite large in a linear collider. Collimators placed near the beam to intercept the halo particles can be damaged or destroyed by the high beam power density of the core if the beam is inadvertently steered onto a collimator.

Although the parameters of the NLC BDS are far beyond anything that has been achieved in a storage ring, the Stanford Linear Collider (SLC) [1] demonstrated the viability of a fully-integrated linear collider beam delivery system with millimeter-sized betatron functions and routine collision of beams with rms sizes of under 1 μm. The Final Focus Test Beam (FFTB) [2] at SLAC was a single-beam demonstration of a linear-collider beam delivery system with IP betatron functions comparable to the NLC; vertical beam sizes of 70 nm were routinely achieved. The NLC BDS design is based upon experience from these two facilities. In addition, a vigorous R&D program on passive and active magnet position stabilization, ground

motion, materials damage thresholds, and instabilities driven by collimators close to the beam have all yielded insights which have been incorporated into the design of the system. In all particulars, therefore, the NLC BDS design is based upon the performance of previous accelerator systems or the results of R&D.

In the remainder of this chapter, the design of the NLC Final Focus and the SLC and FFTB results relevant to the Final Focus are presented, followed by the status of the collimation system design, the chosen layout for incorporation of all the components, and the possibility of constructing a beam delivery system engineering test facility.

6.2 Final Focus

As described in the Introduction, the role of the final focus is to reduce the size of the beam at the IP sufficiently to provide the required luminosity. Because of the relatively low collision rate of the NLC – one bunch train each of electrons and positrons is delivered every 8.3 milliseconds – the beams must be reduced to extraordinarily small sizes. RMS beam sizes at the IP of 245 nm (x) by 2.7 nm (y) are required to achieve luminosity of 2×10^{34} $cm^{-2}s^{-1}$ at 500-GeV cms. The small beam sizes are achieved by generating beams with small normalized emittances – 3.0 x 0.02 mm-mrad – which are preserved throughout the injector, main linac, and BDS regions, and by using strong quadrupole magnets at the end of the final focus to reduce β^*_{xy} to 8 x 0.1 mm.

The challenges for the final-focus design are fourfold. First, the final focus, like other parts of the NLC, must minimize emittance dilution due to misalignments, errors of beam line components, and synchrotron radiation. Second, the final doublet quadrupoles which generate the small β^* values introduce a large energy-dependent focusing, or chromaticity, which must be corrected. Otherwise, the finite energy spread of the beam would cause the beam size at the IP to be much larger than that expected, given the emittances and betatron functions. Third, the aberrations that are typically introduced by the nonlinear elements that correct the chromaticity must be minimized. Fourth, the very small beams at the IP must be kept in collision with one another; a motion of one beam relative to the other of a few nanometers is sufficient to measurably reduce the luminosity.

6.2.1 Correcting the Chromaticity

Correcting the chromaticity of the final doublet is the issue that drives the rest of the design. In the final-focus systems used at the SLC and the FFTB, which were also the basis of the 1996 ZDR final-focus design, the chromaticity correction was accomplished in dedicated 'chromaticity correction sections.' In these sections, a combination of bend magnets and sextupoles generated a chromaticity equal-and-opposite to that of the final doublet. The primary design limitation in these systems was that the energy loss from synchrotron radiation between the last sextupole and the IP had to be minimized, to avoid causing a breakdown of the chromaticity correction. Because of this requirement the bending magnets were weak, and the final focus was correspondingly long.

The ZDR design called for a 1.8-km-long final focus that was capable of handling up to 750-GeV beams, but that would need to be over 3 km long for 2500-GeV beams. In the present design [3], this limitation is addressed by interleaving the chromatic correction sextupoles with the final doublet quadrupoles. This configuration requires a horizontal dispersion through the final doublet, which is tuned to be exactly zero at the IP; the large dispersion in the strong doublet quads introduces additional aberrations that must be cancelled. Nonetheless, the resulting configuration is both simpler and shorter than previous final-focus systems: less than 0.4 km is required for 750-GeV beams and 0.8 km will handle 2500-GeV beams. A schematic of the present design concept is shown in Fig. 6.1, and a plot of the optical functions is shown in Fig. 6.2. The energy reach of the final focus is shown in Fig. 6.3.

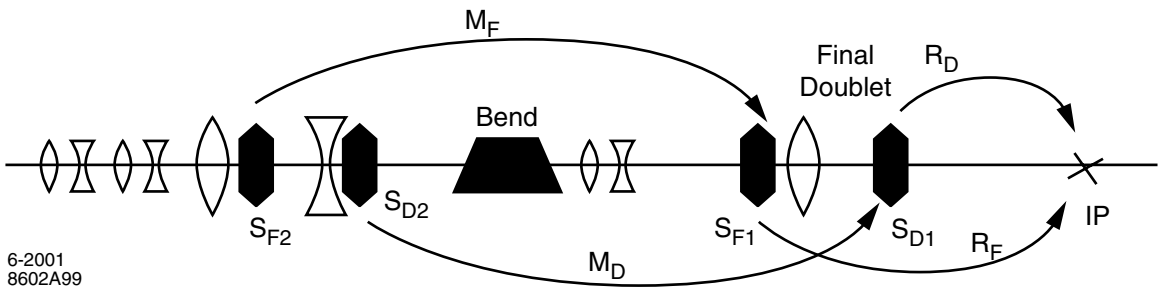

Figure 6.1: Schematic design of the current NLC FF.

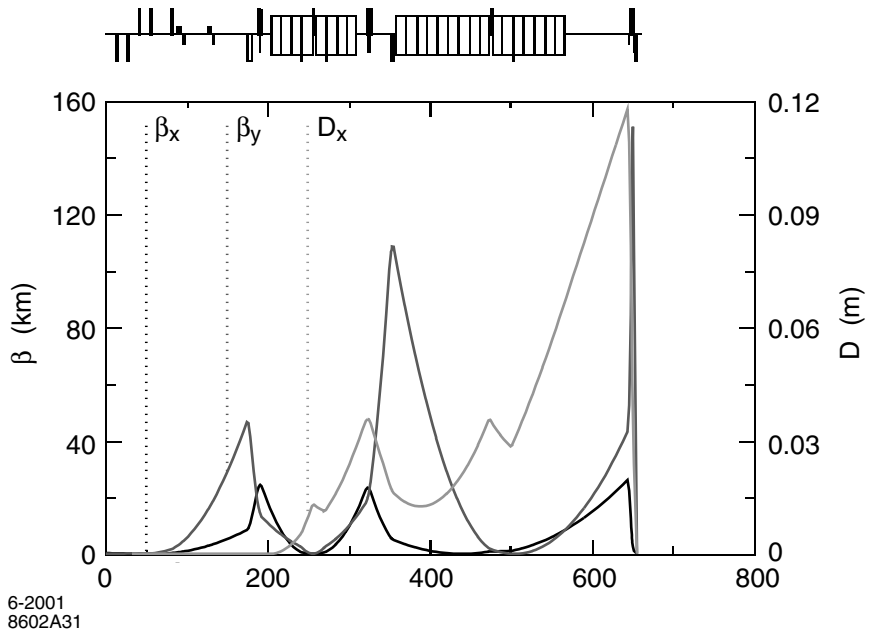

Figure 6.2: Optics of the NLC FF.

6.2.2 Additional Aberrations

Once the chromaticity of the final focus is corrected, the principal aberration to be cancelled is generated by the sextupoles that are required for chromaticity correction. This is accomplished by placing additional sextupoles in the beamline, with optical transformations between sextupoles which cause the geometric aberrations of the sextupoles to cancel while the chromatic aberrations remain, as shown in Fig. 6.1. In the SLC and FFTB, each of the sextupoles in a matched pair contributed 50% of the chromaticity correction. The combined effect of the chromaticities of the sextupoles, the quads between the sextupoles, the quads between the last sextupole and the final doublet, and the doublet chromaticity caused these designs to provide correct focusing for only a narrow range of particle energies. A more recent design by Oide [4] ameliorated this limitation by generating as much of the chromaticity correction as possible in the sextupoles closest to the IP, rather than splitting it equally among the pairs of sextupoles in a given family. The present design of the NLC final focus combines an extreme form of Oide's asymmetric-chromaticity solution with placing the chromaticity correction sextupoles in the final doublet itself. The combination of these features

minimizes the chromatic aberrations of traditional final-focus systems. Fig. 6.4 shows the luminosity as a function of fractional energy error for the ZDR and present NLC final-focus designs. The performance of the two is comparable, but the new system's performance is a smoother function of energy, indicating weaker chromatic aberrations. Another valuable attribute of the system is that off-energy particles tend to have small amplitudes in the final doublet magnet, whereas traditional final-focus systems tend to drive off-energy particles to very large amplitudes in the final doublet. This is shown in Fig. 6.5.

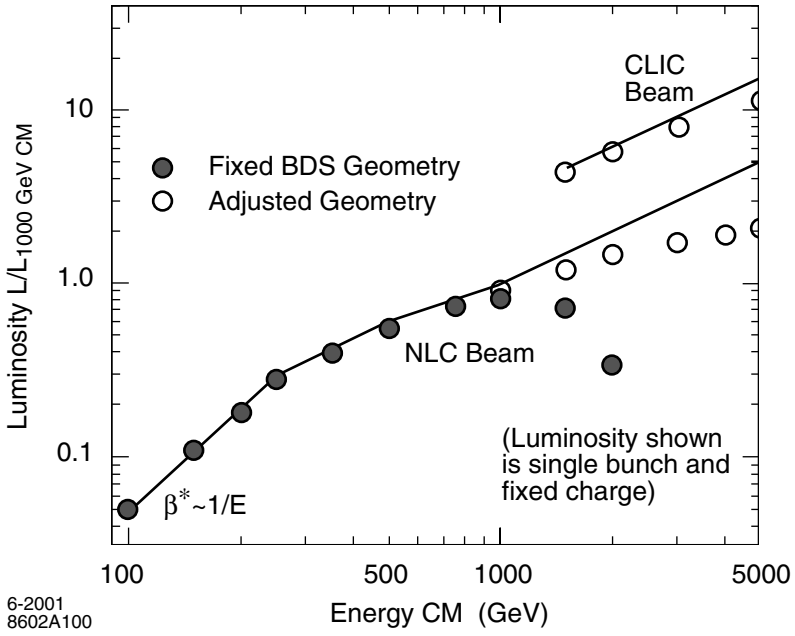

Figure 6.3: Energy reach of the NLC final focus. The present system, with under 1 km total length per side, can accommodate center-of-mass energies up to 5 TeV. Because of synchrotron radiation effects, the bending angles in the final focus must be reduced for CM energies above 1 TeV. Also shown is the luminosity if the normalized emittance delivered by the injector can be reduced at higher energies, as assumed in some studies of multi-TeV linear colliders.

6.2.3 Jitter and Emittance Dilution Tolerances

A critical issue for all NLC beamlines is whether or not the tolerances that must be kept are realistic. The most severe tolerances are magnet alignment and position stability. Magnet field quality and power supply stability tolerances are also important, but in general these tolerances are comparable to those achieved at the FFTB. Figure 6.6 shows the magnet position drift and position jitter tolerances for the NLC FF. The difference between 'drift' and 'jitter' is one of effect: drift tolerances are the tolerances which must be held to maintain small beam spots, while jitter tolerances are the ones which relate to maintaining collisions of the very small beams at the IP. Although the tolerances in Fig. 6.6 are small, it is important to note that these are so-called 'bare' tolerances – tolerances in the absence of feedback systems or other noninvasive correction algorithms which can stabilize accelerator performance. Understanding the real performance of the final focus requires simulation studies that include the planned diagnostic and correction systems, and their algorithms. This is discussed in greater detail in Chapter 7, but a few key examples are considered here.

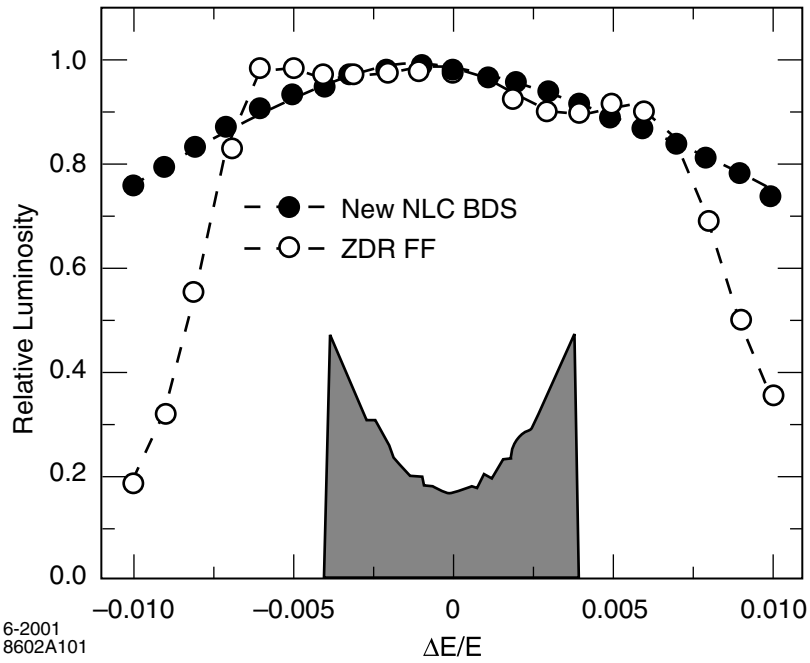

Figure 6.4: Energy bandwidth of the FF at the IP. Both ZDR-era and present final focus designs are shown. The natural energy distribution of the beam from the NLC main linac is also shown.

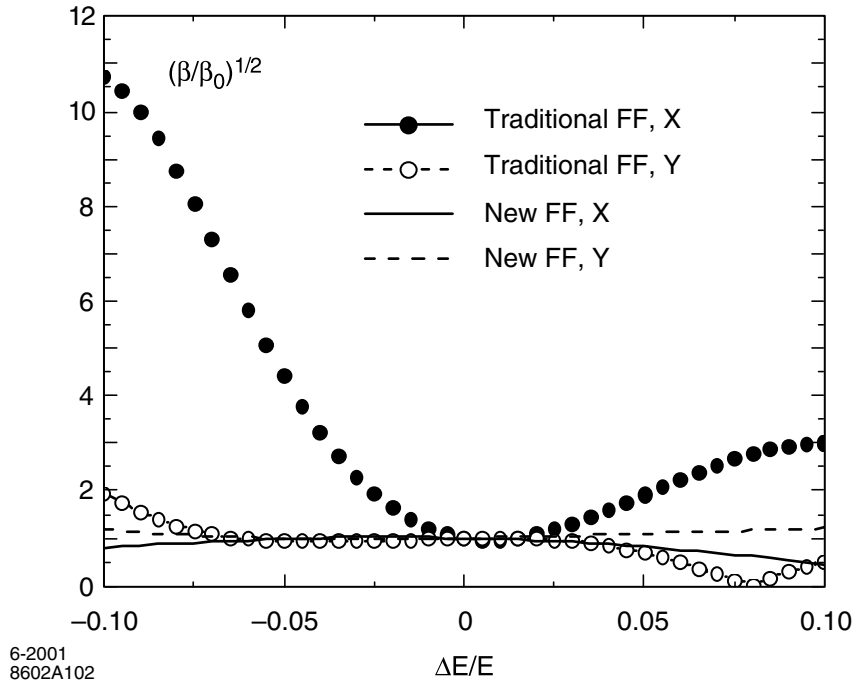

Figure 6.5: Energy bandwidth of the FF at the final doublet.

Drift Tolerance and Performance: One of the most serious potential sources of emittance dilution is beam line magnet misalignments driven by diffusive ground motion. Figure 6.7 is the result of a simulation that misaligns the elements of the 1-TeV cms NLC BDS configuration according to the 'ATL law,' which describes the effect of this ground motion. Here the mean-squared relative motion of two elements is proportional to the product of the distance between the points (L) and the time that has ensued (T). The constant A varies with the local geology and for this simulation is assumed to be 5×10^{-7} $\mu m^2/m/s$, which is the ATL coefficient derived from recent ground-motion measurements at SLAC. The curves show that luminosity would degrade under ATL motion in approximately 2 minutes if only the beam-beam deflection collision stabilization feedback was present. If in addition orbit control feedback is allowed to steer the beam through the centers of critical quadrupole and sextupole magnets, the time for luminosity degradation increases to approximately 1 day. Finally, if direct optimization of the main aberrations via global knobs is added to the system, the luminosity lifetime increases to several months, after which a disruptive realignment procedure would be required.

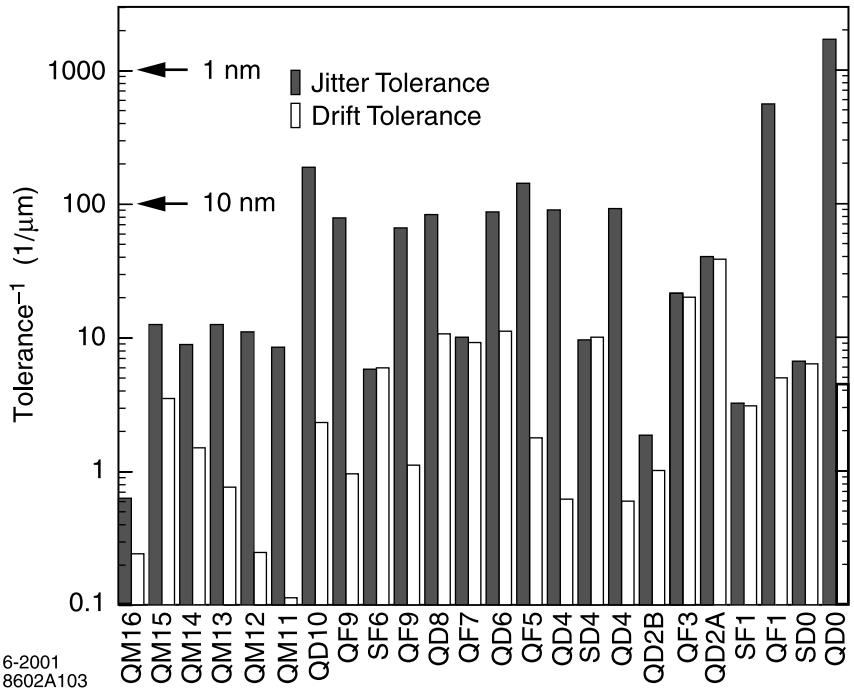

Figure 6.6: Magnet position jitter and drift tolerance of the NLC FF. 'Jitter' tolerance relates to the magnet's capacity to steer beams out of collision at the IP, while 'drift' refers to the magnet's capacity to cause the beams at the IP to be too large. Reciprocal tolerances are shown, so in this case bigger is worse. Note the large jitter sensitivity of the final doublet magnets QF1 and QD0.

Jitter Tolerance and Performance. Figure 6.6 shows that typical jitter tolerances in the final focus are on the order of 10 nm. Although such tolerances are tight, the situation is not as grave as might naively be expected. In particular, the tolerances in Fig. 6.6 are for incoherent motion of the magnets. The sensitivity of the luminosity to correlated motion is much smaller. As discussed in Chapter 7, the natural characteristics of ground motion are that low-frequency motion, which typically accounts for hundreds of nanometers of rms motion, is highly coherent, while high-frequency motion, which is nearly incoherent, accounts for only a few nanometers of motion. This means that if the magnets are supported in such a way that their motion is identical to the motion of the underlying ground, the luminosity loss from jitter of

the quads upstream of the final doublet will be only a few percent. In section 6.2.4, a proof-of-principle magnet support which achieves this goal is discussed. Thus, the tight jitter tolerances of the magnets upstream of the final doublet are not considered a serious limitation on the performance of the final focus.

As Fig. 6.6 shows, the jitter tolerances of the final doublet quadrupoles, QD0 and QF1, are roughly an order of magnitude tighter than those in the rest of the final focus. The final doublet quads are the only ones in the NLC that cannot meet their tolerances through passive stabilization. An additional constraint on the doublet magnets is that they must be mounted within the detector, as shown in Fig. 6.8. Jitter suppression for these magnets must include a combination of passive and active methods. Passive methods include locating the IR hall sufficiently far from cultural sources of vibration, minimizing potential vibration sources under NLC control through proper engineering, and engineering to ensure the detector, magnet technology, and doublet support girders are stable and do not amplify motion. There are R&D programs in active vibration suppression technologies in three different areas: measurement of motion through optical interferometers or accelerometers; active motion control at the nanometer level using piezoelectric or electrostatic movers; and a high-bandwidth beam-based feedback that can correct beam-beam offsets within a single bunch train. It is expected that a combination of passive and active magnet stabilization technologies will provide the jitter control required in the final doublet, and that the high-bandwidth feedback can provide an additional margin of safety and protection against small step-function changes in the accelerator.

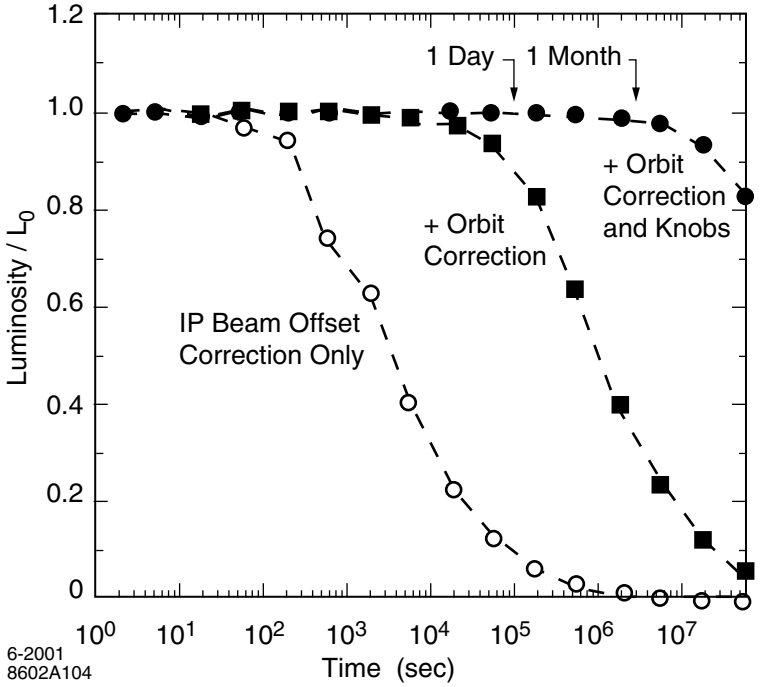

Figure 6.7: Degradation of alignment under ATL ground motion with IP beam-beam deflection based feedback only, with orbit feedback added, and with direct luminosity optimization added.

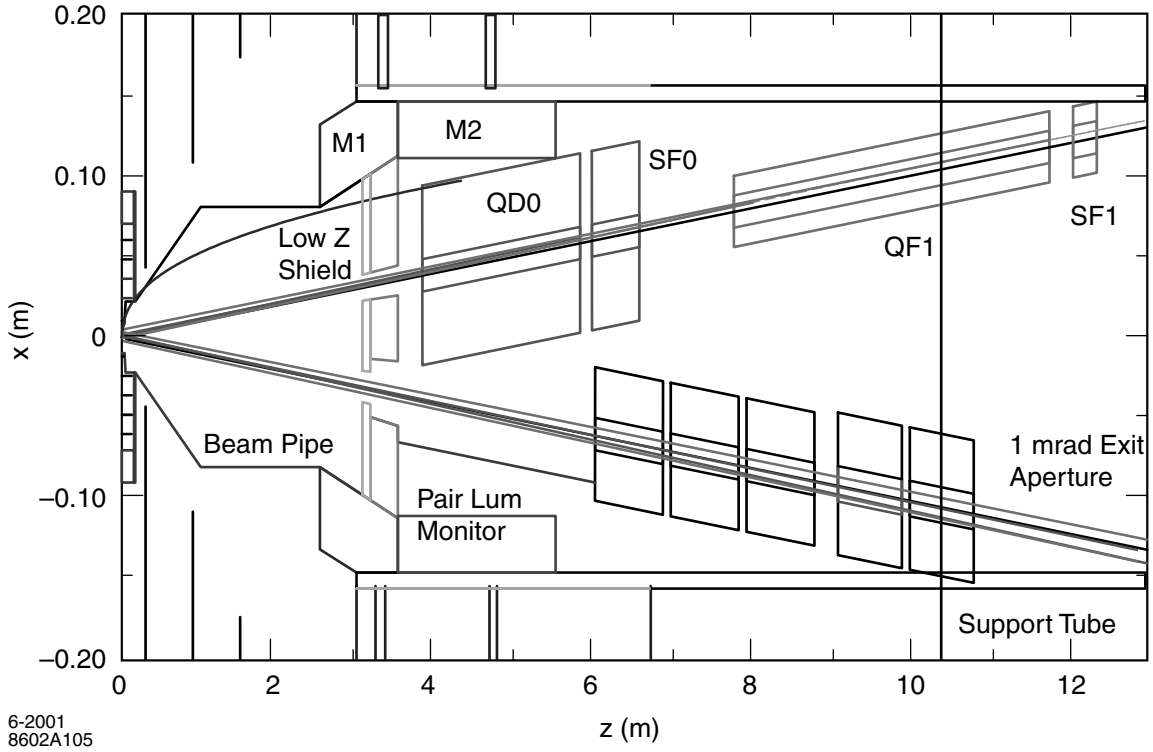

Figure 6.8: The IR layout for the NLC Large Detector.

6.2.4 FFTB and SLC Experience

The Final Focus Test Beam (FFTB) was a linear collider final focus scaled to the SLAC 47-GeV beams. The FFTB was designed to generate β^* values of 10 x 0.1 mm, almost identical to the design values of the NLC. Given the normalized emittances available from the SLAC linac, this would result in rms beam sizes of 1.7 μm by approximately 45 nm at the IP. This would provide a test of the optics designs, tuning techniques, and diagnostic and correction hardware required for the NLC final focus. The actual measurement of a 40-50 nm rms vertical spot size in the FFTB was complicated by both linac-induced incoming beam jitter and the experimental limitations of the laser-interferometer beam size monitor. Figure 6.9 shows the rms vertical beam spot size as measured, with a mean value of 70 ± 1.5 nm. When the beam emittance, betatron functions, jitter between beam and laser interferometer, and the estimated effects of limited tuning precision are folded in, the expected beam size was 58 ± 8 nm, 1.5 σ from that observed.

Each quadrupole and sextupole in the FFTB was mounted on a magnet mover system based on rotating eccentric cams capable of adjusting its position in 300-nm step sizes. Each quadrupole also incorporated a BPM with 1 μm resolution. These sat upon Anocast magnet supports grouted solidly to the sandstone underlying the FFTB tunnel floor. The magnet alignment procedure relied upon beam measurements to achieve a precision beyond the capabilities of conventional surveying and mechanical alignment techniques. Figure 6.10 shows that the alignment resolution achieved was 1-10 μm with the decrease in precision at the end of the beam line due to the lack of BPMs further downstream. Chapter 7 will discuss how this procedure, using movers with a smaller step size of 50 nm and BPMs with 300 nm resolution, will be used to align the NLC linac quadrupoles to a tolerance of 2.5 μm.

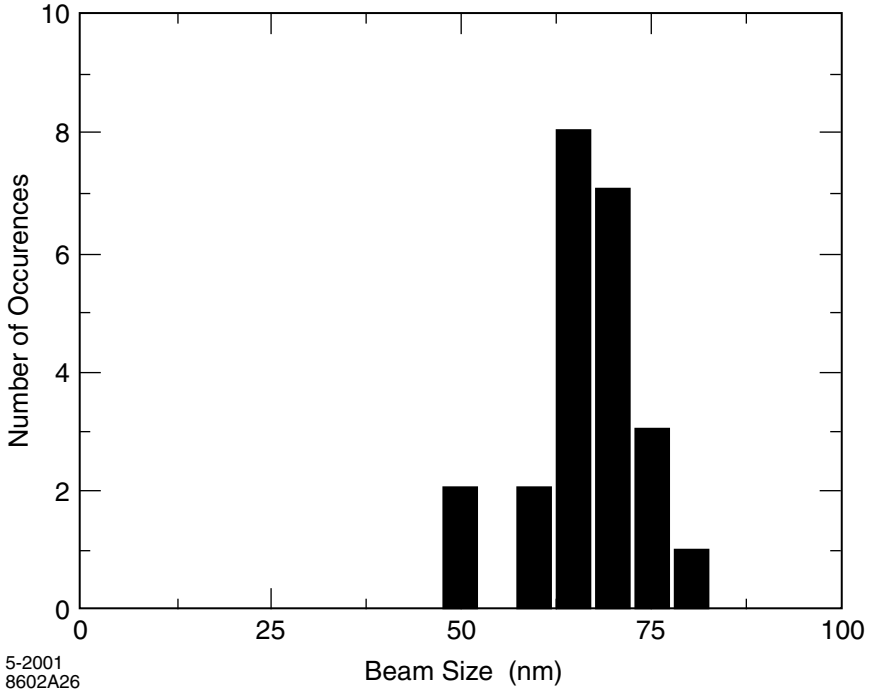

Figure 6.9: Spot size measurements at the FFTB.

Many of the engineering issues relevant to stable operation of the FF were investigated at FFTB. Tunnel temperature variation, airflow, and the impact of vibrations caused by flowing magnet-cooling water are examples. Figure 6.11 shows the integrated power spectra of geophones, one of which was mounted on the tunnel floor, and one atop a typical fully powered FFTB quadrupole with cooling water flowing, along with the difference between the magnet motion and the motion of the nearby ground. Above the 3 Hz signal-to-noise cutoff of the geophones used in this measurement there are only 2 nm of relative motion. The performance of the FFTB magnet supports is quite close to that required for NLC quadrupoles.

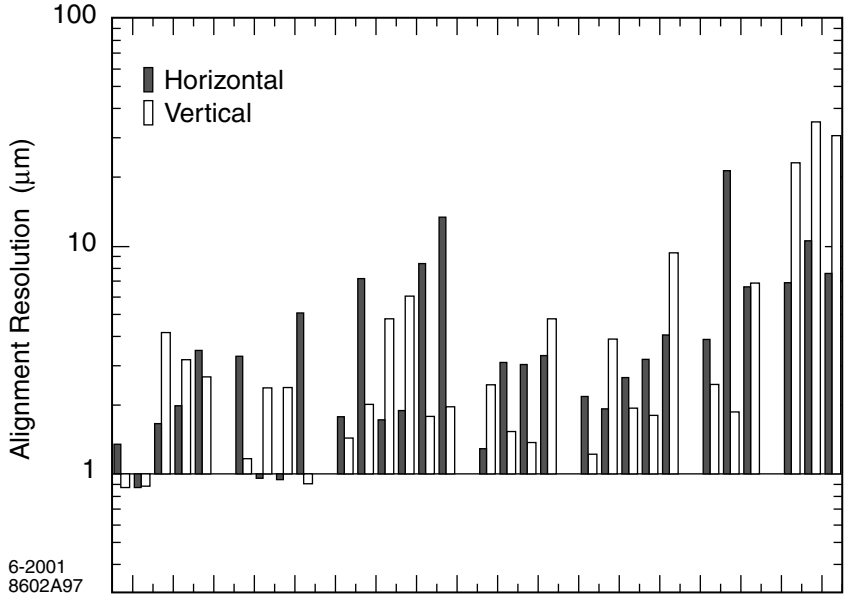

Figure 6.10: The horizontal and vertical alignment precision of quadrupoles in the FFTB after beam-based alignment.

The Stanford Linear Collider (SLC) was the first linear collider, and it operated at the energy of the Z^0 boson from 1989 through 1998. The SLC is to date the only facility that routinely collided submicron beams and demonstrated the integrated operation of all the components of a linear collider. Figure 6.12 shows the reconstructed vertical position of $Z^0 \rightarrow$ hadron events recorded by the SLD vertex detector over a period of approximately 10 days in 1997. The Z^0 events are binned in groups of 30 and the mean y for the group plotted versus time of day. The luminous region for the SLC is approximately 0.5 μm in vertical extent, and Fig. 6.12 shows that over the course of 1 day its vertical position varies by 40 times this distance. Nonetheless, the collision steering feedback keeps the beams centered on each other, and other feedback systems to control the trajectory and optimize the luminosity maintain a steady Z production rate over the entire period.

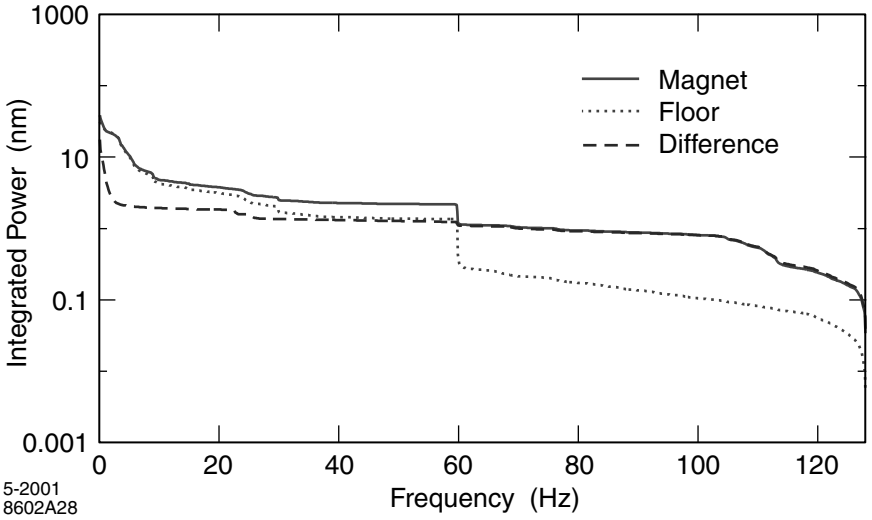

Figure 6.11: Integrated power spectrum from the vibration of a fully powered FFTB quadrupole with cooling water running. The additional rms motion of the magnet with respect to the tunnel floor is 2 nm.

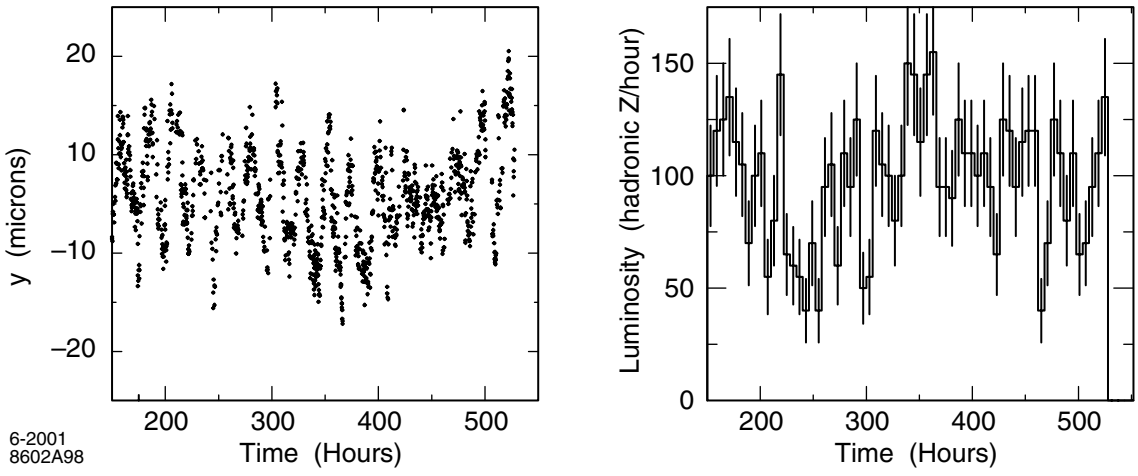

Figure 6.12: Average reconstructed vertical position of $Z^0 \rightarrow$ hadron events in the SLD and the measured SLC luminosity over a 10-day period.

6.3 Collimation System

The level of backgrounds the SLD detector could tolerate often limited luminosity at the SLC. It is well understood that the backgrounds were due to synchrotron radiation (SR) photons, produced by the beam halo in the final lens system, hitting masks near the IP. Ray tracing studies of the NLC final focus have shown that this is a potentially serious source of backgrounds for the Linear Collider Detector (LCD) as well. Because of the very high beam energy at NLC, the SR photons generated in the final doublet tend to have high energies as well, which makes it untenable to use masking in the IR to shield the detector from these SR photons. Consequently, the NLC collimation aperture is determined by the maximum amplitude with which a particle can pass through the final doublet without emitting SR photons that hit the detector. According to tracking studies, particles which pass through the IP with horizontal angles under 240 microradians, and vertical angles under 1000 microradians, will not produce SR backgrounds in the final doublet. Note that these limits are significantly tighter than would be required to protect the final doublet vacuum chamber from direct impact of primary particles; the SR envelope sets the collimation aperture, not the beam-pipe radius.

Collimation of the NLC beam requires putting material very close to beams with high energy density, which in turn creates a risk that a missteered beam might destroy the collimator. Indeed, protection of the detector from such a beam is a secondary function of the BDS collimation system. In principle, the collimators can be protected from damage by enlarging the beam's transverse dimensions at the collimator locations, but this requires an optics which is itself chromatic and can generate more halo particles. In practice, in order to limit the betatron functions in the collimation region, the design relies on thin (0.25-0.5 radiation length) devices called spoilers which scrape the halo and which, if accidentally struck by the full power beam, will enlarge the spot size via multiple coulomb scattering. The scattered halo and enlarged beam are then stopped on thick (20 radiation length) absorbers. Although the damage threshold of the spoilers is considerably higher than that of the absorbers, the design outlined above still requires an enlarged beam size at the spoiler location if the spoiler itself is to survive damage from an errant bunch train. An additional concern is that spoilers close to the beam may introduce transverse wakefield deflections which would unacceptably degrade the beam quality at the IP.

The number of particles that may be absorbed by the collimation system, and the efficiency with which they are stopped, are both determined by the production and transport of muon secondaries from the collimation process. Simulation studies have shown that as many as 10^9 primary electrons or positrons per train can be removed by the collimation system without producing an unacceptable muon flux in the detector, although this number depends somewhat upon the exact configuration of the beam line. The number of primary particles that can be stopped close to the detector without unacceptable muon production is only 10^4.

Based on the considerations above, the requirements of the collimation system can be elucidated. The collimation system optical design must enlarge the beam sufficiently to allow the placement of enough survivable collimation devices to reduce the halo by 5 orders of magnitude. It should allow for potentially frequent off-energy beam trains and occasional orbit variations from equipment failure or operator error. The design must not require tolerances that might lead to emittance growth or collimation apertures so small that their wakefields induce unacceptable beam jitter. The collimators themselves must be made of materials thin enough or robust enough to withstand both the constant beam halo and the occasionally errant beam pulse. Their surfaces must have sufficient smoothness, low enough resistivity, and be shaped so as to produce minimal wakefields. The mechanism that controls the collimator jaw placement must provide adequate control of the gap and its alignment.

6.3.1 Collimation System Design

The design of the NLC collimation system has evolved significantly since the 1996 ZDR. At that time the system required a 2.5-km-long beamline to enlarge the beam envelope to such large values that the spoiler systems that removed the beam halo could be guaranteed to survive the occasional errant beam pulse. This requirement put very challenging tolerances on both jitter and the betatron phase matching of certain magnets.

The collimator system currently in the baseline design consists of an upstream energy collimation, based on a dogleg bend and accommodating the linac tune-up beam dump, followed by a betatron collimation system. Because klystron trips causing off-energy beams may be relatively frequent events, and can occur with only microseconds of warning, the energy collimators are designed to be capable of surviving contact with a bunch train. The system combines a large horizontal dispersion and a large vertical betatron function to ensure that the transverse size of beam pulses at the 0.5 radiation length spoilers is large enough that the charge density is below the damage threshold. Multiple coulomb scattering in the spoiler further increases the beam size before the pulse is stopped in an absorber downstream. The betatron collimation system downstream scrapes the beam halo and provides machine protection against infrequent orbit disruption of on-energy beams. Based on the SLC experience, very few of these events are expected to occur in each run. A lattice with more relaxed tolerances has been designed that uses as its basis the concept of 'consumable spoilers.' These are cylindrical spoilers or scrapers that can be rotated to present a clean surface to the beam if damaged by an errant pulse. Their circumference is such that approximately 1000 damaging pulses can be permitted before replacement is necessary. Tracking studies indicate that this system gives the 5 orders of magnitude of halo reduction required.

A recent development in the collimation system is the use of octupole doublets which permit the beam halo in one betatron phase to be reduced in amplitude, while leaving the beam core nearly unaffected. A pair of these doublets has been shown to reduce the halo in the critical final doublet betatron phase by a factor of 4, which in turn would permit equivalently larger collimator apertures in that phase, as shown in Fig. 6.13. This would also dramatically decrease the impact of collimator wakefields, as the wakefields are believed to scale with the inverse square of the gap size. Future modifications to the lattice are under study which integrate the collimation into the final focus, exploiting the increased energy bandwidth and dynamic aperture of the current final focus and also permitting straightforward chromatic correction of the collimation system. These developments suggest that the collimation system will ultimately no longer be a concern, from the point of view of BDS performance.

6.3.2 Spoiler Design

The concept of consumable spoilers was introduced in the previous section. Although the use of thin spoilers to enhance protection of downstream components has been used in some limited applications in existing accelerators, the NLC collimation application is unique in many aspects. The NLC spoilers have tight positioning accuracy tolerances, the gap size and gap-center position must be maintained when the spoiler surface is advanced after damage has occurred, and the transverse wakefields from the spoilers must be acceptably small. A further complication is that the NLC spoiler must operate reliably under high vacuum and in a high-radiation environment. Because of these issues, the collimation system spoiler has been the subject of a substantial research program [5].

There are four elements in the baseline design R&D program. The first is the fabrication of a prototype consumable spoiler to investigate the engineering challenge of providing accurately aligned surfaces in a piece of moving machinery that must operate under vacuum. A configuration in which each collimator jaw is a rotating wheel has been selected due to its overall compactness. Figure 6.14 shows a photograph

of the prototype device, a drawing to schematically indicate how it operates, and a plot showing, as an example, its ±15 μm gap width stability under rotation. This prototype has pointed the way to minor design modifications and demonstrated that collimation devices of this type can be incorporated reliably into any final system design.

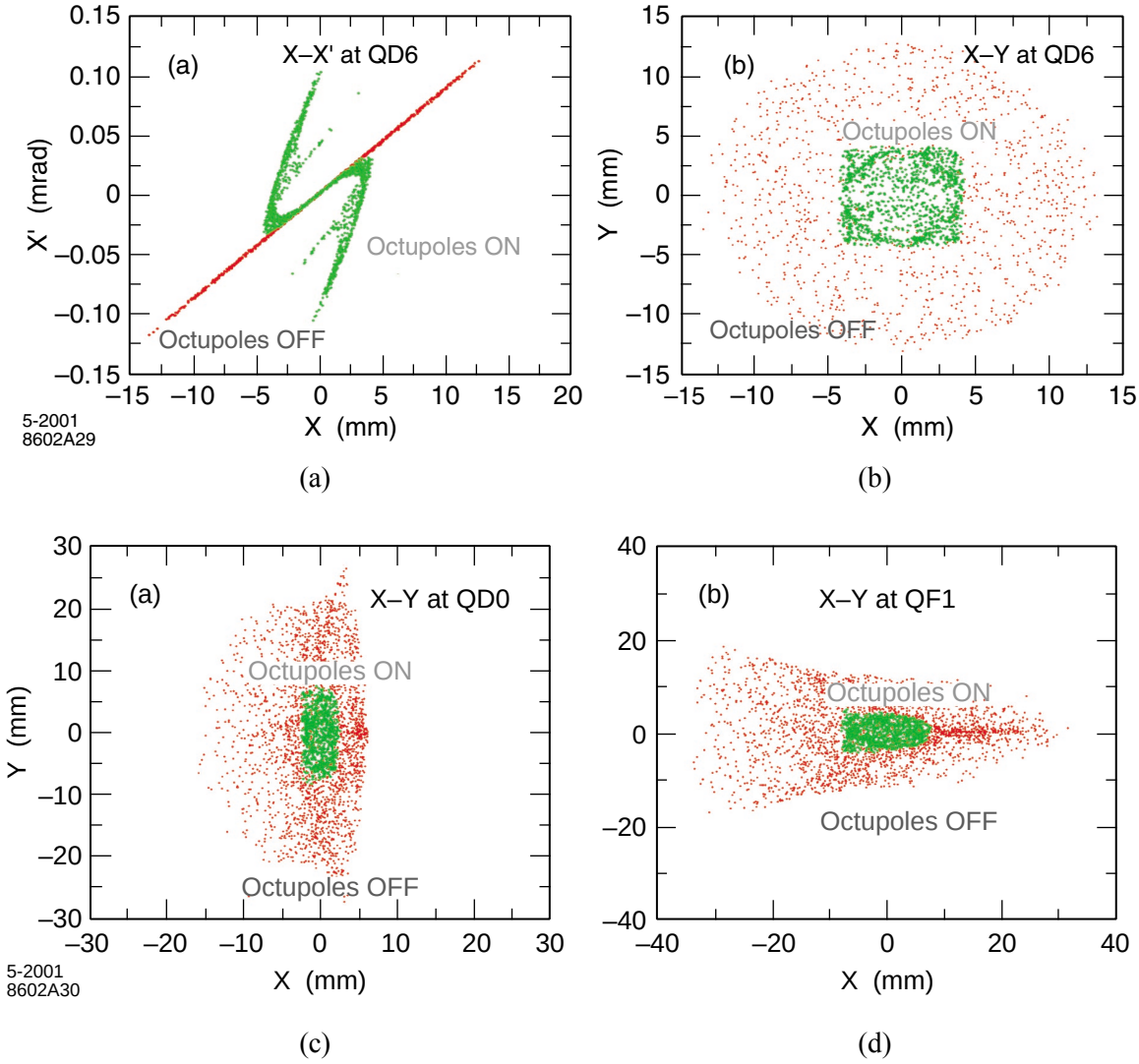

Figure 6.13: Simulation of tail folding by means of two octupole doublets in the new NLC final focus. The top figures show the phase space after a drift following the octupole doublets. The bottom figures show the beam distribution in the final doublet. The input beam has a flat distribution with half width (X, X', Y, Y') = (14mm, 1.2mrad, 0.63mm, 5.2 mrad) in IP units and ±2% energy spread. This corresponds to approximately (65, 65, 230, 230) sigma with respect to the nominal NLC beam.

The second R&D effort is an attempt to use solidifying liquid metal as the basis of a collimator design. In this scheme, the collimator wheel would pass through a bath of liquid metal where it is coated by a thin layer that is pressed onto it by a second roller. The material studies phase of this project is finished and a

proof-of-principle prototype has been built based on niobium and molybdenum wheels with tin as the liquid metal. The prototype has yielded very smooth surfaces and pointed out a number of design challenges. If successful, such a collimator could be put so close to the beam that it is damaged by beam image current heating at every pulse and yet be constantly rotated and repaired. Such a collimator would technically be 'renewable' rather than 'consumable,' and would provide more options for lattice design that could potentially further reduce the required tolerances.

The third element of the collimator R&D effort is a series of beam damage experiments [6]. Samples of various materials have been exposed to single shots of 30-GeV beam of 3-20 x 10^9 electrons with rms transverse areas of 50-200 μm^2 at FFTB. The samples were then inspected to understand the resulting damage. To date, thin samples of copper, nickel, titanium, and tungsten-rhenium alloy have been tested. The tests have indicated that, for targets which are less than 1 radiation length in thickness, the damage threshold which is calculated by naively equating the thermal expansion stress of the material to its yield stress is a considerable underestimate of the instantaneous heating which the materials can tolerate. This is believed to be due to the fact that in thin targets the heated material is not fully constrained, and so the thermal expansion stress can be relieved by the heated material 'bulging' from the front and back surface of the target. Further tests of samples that more completely approximate an NLC spoiler are planned.

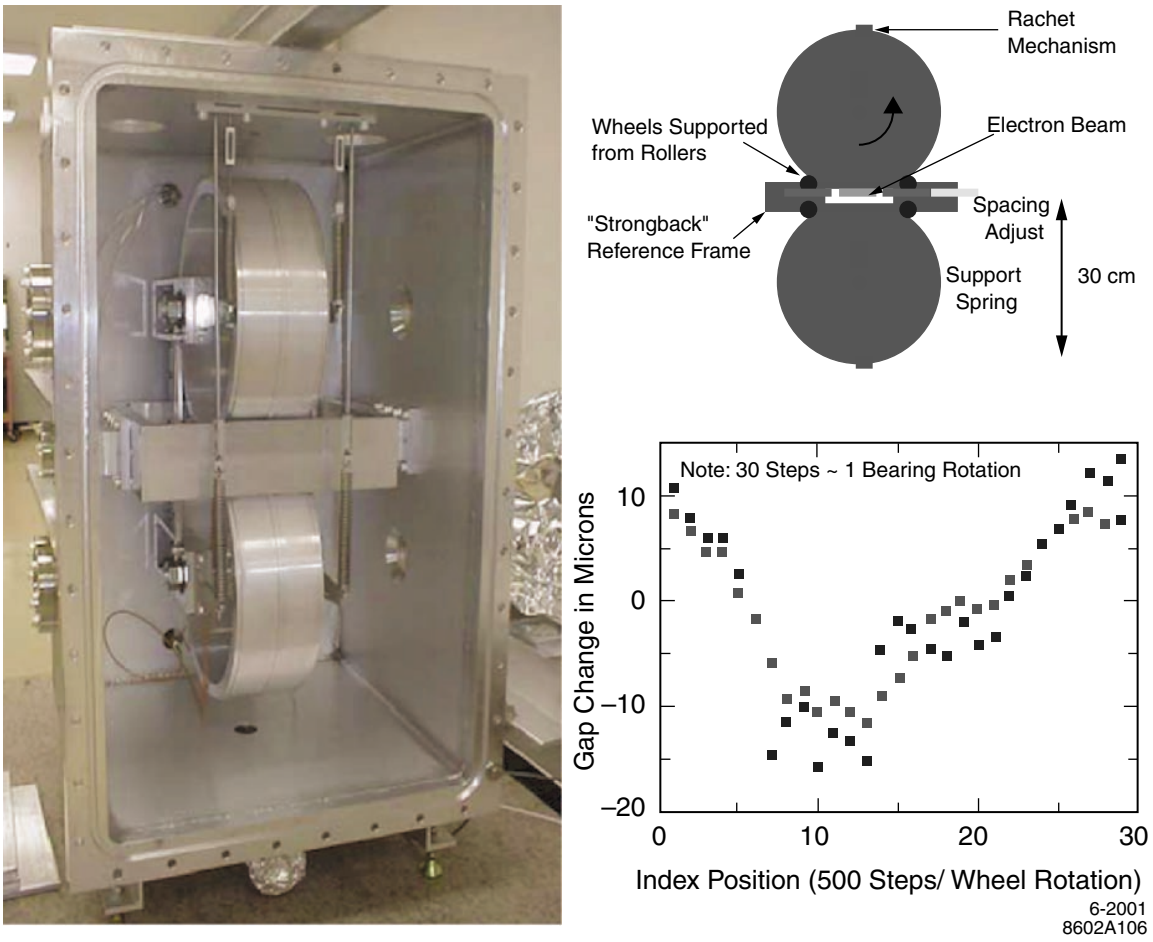

Figure 6.14: Rotating consumable collimator prototype.

The fourth element of the collimation system R & D effort is a series of experiments [7] meant to fully explore the impact of collimator wakefields. In the baseline collimation lattice the collimator gaps are on the order of 200 μm x 200 μm. Wakefield effects due to collimator shape, resistivity or smoothness may produce enough jitter amplification to adversely impact luminosity. A first set of measurements has been performed on a set of tapered copper collimator jaws to study the geometric wakefield of such objects. A moveable vacuum enclosure holding four collimator samples plus a standard large-diameter round beam pipe has been installed at the SLAC linac near the ASSET test area. The wakefield kick applied to the beam is measured by BPM arrays as a function of beam location for each collimator and the results compared to analytic and numerical estimates. Figure 6.15 shows the elevation and beam's eye view of the first set of four samples tested along with an example of data taken.

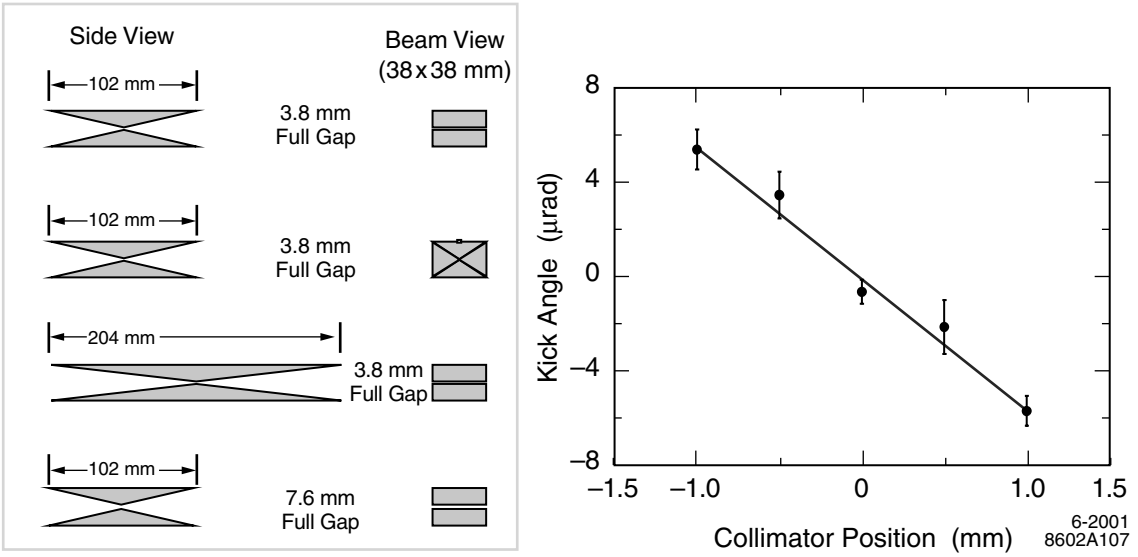

Figure 6.15: Collimator Wakefield Experiment results.

Table 6.1 compares the measurement results with analytic theory and simulations. When this series of experiments was originally planned, the only analytic theory available was that labeled 'long taper' in Table 6.1. The results are all much smaller than these predictions and the discrepancy has led to the development of an additional theoretical model applicable in the short taper regime. Both the collimators used in the tests and the eventual NLC collimators will probably fall in between the regions of applicability of the two models and theoretical work to bridge the gap is ongoing. Future tests will focus on the resistivity of the collimator material, where graphite and titanium samples will be compared against copper, and on surface roughness.

Table 6.1: Comparison of Collimator Wakefield Experiments with Theory and Simulation.

SHAPE	ANGLE rad	GAP mm	THEORY SHORT TAPER	THEORY LONG TAPER	MAFIA SIM	ABCI SIM	EXPERIMENT
Flat	0.168	3.8	6.7	30	2.3	-	3.34 ± 0.31
Square	0.335	3.8	13.4	3.7	-	5.6	3.72 ± 0.29
Flat	0.335	3.8	6.7	58	3.1-3.8	-	3.72 ± 0.29
Flat	0.298	7.6	1.7	13	1.0	-	1.44 ± 0.14

6.4 Layout

As described in Chapter 2, a final-focus system operates effectively without modification over roughly a factor of four in beam energy. Its length is determined by the highest anticipated operating energy, since the bend magnets in the lattice must be sufficiently weak to limit SR luminosity loss to a few percent. Above the maximum design energy, the emittance growth is proportional to E^4 and the luminosity falls accordingly. At lower energies the geometric emittance increases, and this causes the beam size in the magnet apertures to increase. Below some minimum energy, the IP beta function must be increased to limit the beam size in the magnet apertures, and the luminosity falls as E^2. Because of the new approach to chromaticity correction described in section 6.2, the final focus is very compact relative to previous designs and scales gracefully to much higher energies. By leaving approximately 800 m of tunnel for the FF, the design can handle center-of-mass energies of up to 5 TeV. Such high energies can only be accommodated in the NLC if other sources of SR luminosity degradation are minimized. Conversely, a final focus which is designed for 500 GeV cms can be as little as 350 meters long and can tolerate substantially more bending over all than a final focus which is designed to accommodate 5 TeV.

The present configuration takes all of the requirements described above into consideration. Two interaction regions are proposed. One interaction region, the HEIR, is free of net bending angles upstream of the final focus. This permits the HEIR to reach extremely high energies. Any bend magnets upstream of the final focus can be reduced in angle while still fitting into the original tunnel. To allow for the 20 mrad crossing angle that prevents parasitic collisions, the linacs are each angled by 10 mrad and are collinear with the beam delivery system tunnels. This is the simplest, least expensive design that can, without additional civil engineering, be used to deliver cms energies up to 5 TeV if required.

The second interaction region, the LEIR, is for use in $\gamma\gamma$ collisions or in e^+e^- collisions up to approximately 1 TeV. The LEIR and HEIR use the same collimation system. Downstream of the collimation is a 25-mrad arc that brings the LEIR beams into collision with a net 30-mrad crossing angle. The HEIR and LEIR have a transverse separation of about 20 m and a longitudinal separation of 440 m, which is achieved by making the beam delivery systems asymmetric in length. This layout allows for seismic isolation of the two IR halls and eliminates the requirement for separate collimation beamlines for each final focus. Tunnel length and installed hardware are minimized in this configuration, as shown in Fig. 6.16. The larger crossing angle of the LEIR is required for the $\gamma\gamma$ option, but 25-mrad bend required to achieve this crossing angle also fundamentally limits the energy reach of the LEIR. There are many other options for the exact configuration of the two IR halls and their supporting beamlines. The selection of a specific design is a balance between the IR hall separation desired, operational issues, and the relative expense of the tunnel lengths and supporting beamlines.

6.5 LINX

The R&D effort discussed above has been fairly modest in scope, involving prototype hardware and limited beam tests meant to answer fairly straightforward questions. Ultimately, the individual components that emerge from the R&D program must be integrated into a beamline and must function properly in that environment. Given the importance of the beam delivery system in the production of useful luminosity, an engineering test facility is planned to validate critical aspects of the design. The final focus of the SLC can, with minor modifications, be run in a mode that serves as just such an interaction region engineering test bed. A Letter of Intent to build and operate this facility, named LINX for LINear Collider X-ing, has been presented to SLAC management and to the NLC Machine Advisory Committee.

Table 6.2 shows the basic parameters of LINX. The three goals of LINX are to test stabilization techniques proposed for future linear colliders and demonstrate nanometer stability of colliding beams, to investigate proposed optical techniques for control of beam backgrounds, and to provide a facility where ultra-small and ultra-short beams can be used for a variety of other experiments. The IP beta functions, bunch charge, and bunch length are identical to those in the NLC 500-GeV cms parameters.

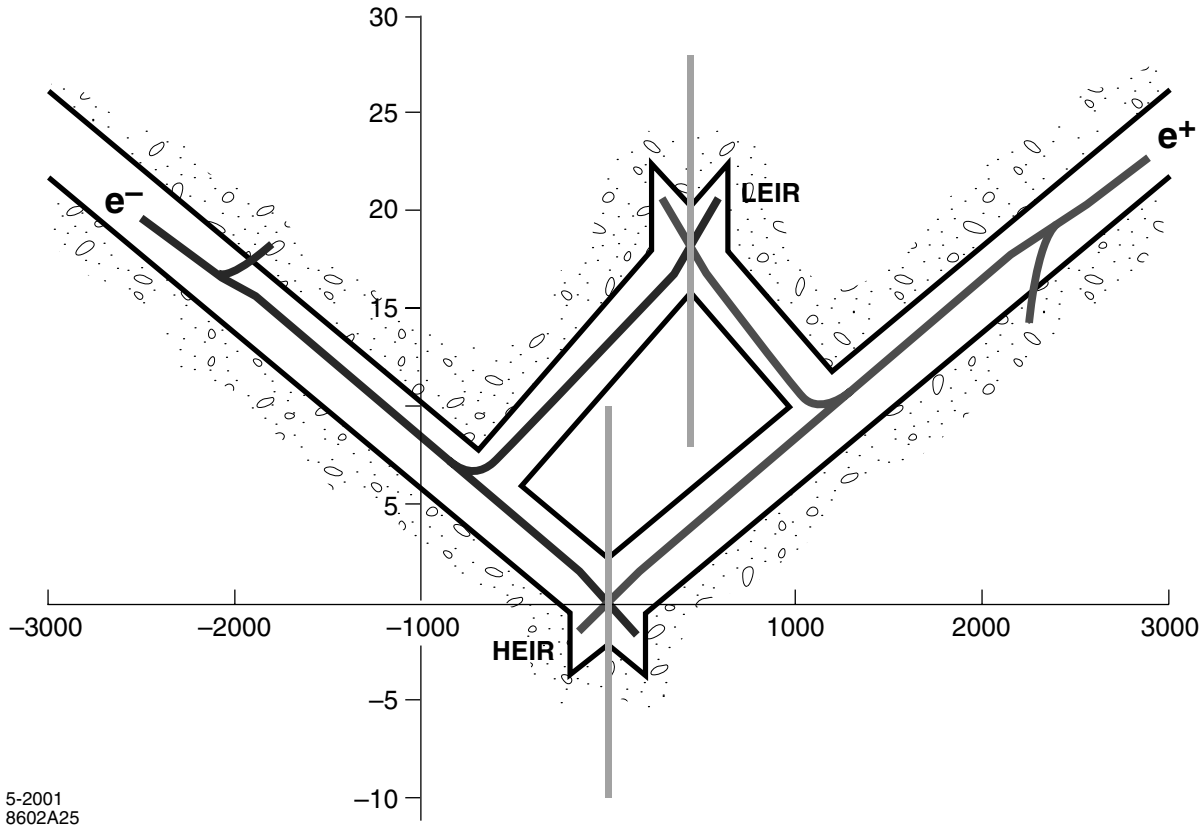

Figure 6.16: Anamorphic layout of the beam delivery system in the NLC 2001 configuration.

The discussion of the FFTB spot size measurement above shows that while the FFTB did achieve the desired betatron functions, 40 nm of beam jitter from various sources must be added in quadrature with the ideal result to explain the observations. A key feature of LINX is that it can achieve 1-nm resolution on the pulse-to-pulse beam-beam jitter by using the beam-beam deflection with beams of from 55 nm to 400 nm in height and 1 μm resolution BPMs. Thus, LINX affords an opportunity to demonstrate the required suppression of beam-beam jitter in an accelerator environment.

Table 6.2: LINX Parameters

Beam energy	30 GeV
IP emittances ($\gamma\varepsilon_x/\gamma\varepsilon_y$)	16/1.6 mm-mrad
IP betas (β_x/β_y)	8/0.1 mm
Bunch length (σ_z)	0.1-1.0 mm
IP spot sizes (σ_x/σ_y)	1500/55 nm
Bunch population (N)	$N = 6x10^9$

The proposed lattice is displayed in Fig. 6.17. Its similarity to that of the NLC FF in Fig. 6.2 is evident. By including an octupole pair in the lattice the concept of using nonlinear optical elements for halo-folding can be experimentally verified. While there is great confidence in the accuracy of the third-order optics programs used to design the FF lattice, detailed experimental conditions, not included in the simulations, sometimes cause less than ideal performance. LINX will provide a basis for confidence in the total integrated beam-delivery system.

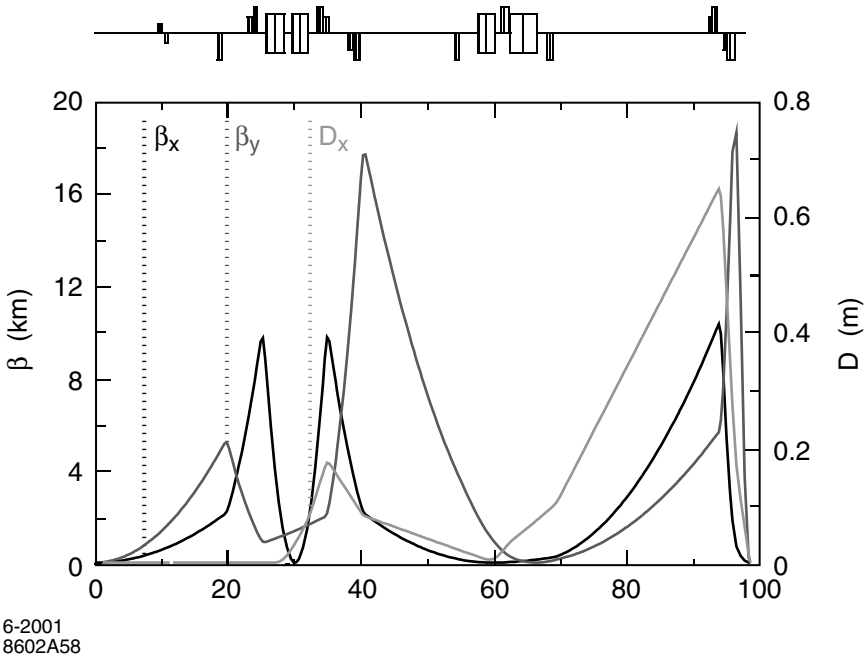

Figure 6.17: Optics of the SLC FF modified according to the new NLC FF design. The final triplets will be replaced by doublets with additional sextupoles interleaved. All the other elements of the SLC FF are left unchanged. One octupole doublet is added for active background control.

References

[1] Brown, K., "Basic Optics of the SLC Final Focus System," *Proc. of the Workshop on Physics of Linear Colliders*, Capri, Italy, 1988, SLAC-PUB-4811, December 1988.

[2] Balakin, V., et al., *Phys. Rev. Lett.*, **74**:2479,1995.

[3] Raimondi, P. and Seryi, A., "A Novel Final Focus Design for Future Linear Colliders," *Phys. Rev. Lett:* **86:**3889, 2001.

[4] Oide, K., "Final Focus System with Odd Dispersion Scheme," *Proc. 15th International Conference on High Energy Accelerators*, Hamburg, Germany, KEK-PREPR-92.058, 1993.

[5] Frisch, J., et al., "Advanced Collimation Prototype Results for the NLC," *Proc. 9th Instrumentation Workshop*, Cambridge, Massachusetts, 2000, SLAC-PUB-8463, June 2000.

[6] Ross, M., et al., "Single Pulse Damage on Copper," *Proc. 20th International Linac Conference*, Monterey, California, 2000, SLAC-PUB-8605, September 2000.

[7] Tenenbaum, P., et al., "Direct Measurement of Geometric Wakefields from Tapered Rectangular Collimators," *Proc. 20th International Linac Conference*, Monterey, California, 2000, SLAC-PUB-8563, August 2000.